communications earth & environment

Article

A Nature Portfolio journal

https://doi.org/10.1038/s43247-025-02475-y

Wildfires will intensify in the wildland-urban interface under near-term warming

Calum X. Cunningham [1] ✉, John T. Abatzoglou [2], Todd M. Ellis[1], Grant J. Williamson [1] & David M. J. S. Bowman [1]

Dangerous fire weather is increasing under climate change, but there is limited knowledge of how this will affect fire intensity, a critical determinant of the socioecological effects of wildfire. Here, we model relationships between satellite observations of fire radiative power (FRP) and contemporaneous fire weather index, and then we project how FRP is likely to change under near-term warming scenarios. The models project widespread growth in FRP, with increases expected across 88% of fire-prone areas worldwide under 1.5 °C warming. Projected increases in FRP were highest in the Mediterranean biome and Temperate Conifer Forest biome, and increases were twice as large under 2 °C warming compared to 1.5 °C. Disaster-prone areas of the wildland-urban interface saw an average of 3.6 times greater projected increases than non-disaster-prone areas, suggesting wildfire impacts will intensify most in regions already vulnerable to dangerous wildfires. These findings emphasise the urgent need to anticipate changes to fire behaviour and proactively manage wildland-urban ecosystems to reduce future fire intensity.

Climate change has increased extreme fire weather globally[1], leading to larger, more intense, and more destructive wildfires[2–4]. Fire intensity, measuring the rate of energy released by the combustion of organic matter[5], is a critical feature of changing fire regimes because intensity influences the degree to which fires can be suppressed, as well as their effects on ecosystems, societies, smoke exposure, and carbon emissions[6–9].

Some regions have experienced increases in fire radiative power (FRP)—a proxy of fire intensity often used by remote sensing studies (e.g.[10])—over the last two decades. This includes a global trend of increasing FRP at night[11], as well as regional increases in FRP in southern Australia, western North America, and most boreal forests[12]. The number of energetically extreme fire events has more than doubled this century globally, with the six most extreme years occurring since 2017[13]. Recent fire disasters with extraordinary property damage and loss of life (e.g., Los Angeles 2025, Valparaiso 2024, Lahaina 2023) have drawn sharp focus on the problem of intense fire intersecting the wildland-urban interface—the area where human development meets wildlands[14]. There is already strong evidence that fire regimes are changing and that fire weather will continue to increase with warming temperatures[15,16], but there is little understanding of how changes in fire weather will affect both fire intensity and exposure of the wildland-urban interface (WUI) to intensifying fire around the world[7].

To address this gap, we developed statistical models of the FRP of active fires observed by MODIS satellites from 2000 to 2023[17], and then projected fire intensity under relatively near-term climate projections. We focused on warming of 1.5 °C above preindustrial levels, corresponding to approximately the next decade or two[18], and 2 °C. These scenarios represent an additional 0.48 °C and 0.98 °C above the period 2000–2023, respectively. They reflect a realistic decision horizon for vegetation management and planning, distinct from abstract, end-of-century predictions, such as the frequently used high-end emissions scenario that involves >4 °C warming by 2100[19]. Predicting near-term conditions also has the benefit that vegetation types and human distributional patterns will be broadly similar to those under which our models of FRP were fitted. This is important because forecasting longer-term vegetation is plagued with uncertainty due to intrinsic climate-vegetation-fire feedbacks[20], uncertain effects of increasing fire frequency such as interval squeeze[21], land cover change from human activities, and the contrasting effects of CO_2 fertilisation and atmospheric drying on plants[22,23]. Short-range projections obviate these uncertainties, as well as longer-term uncertainties in climate models and the emissions pathway we ultimately take.

To project fire intensity, we fit generalised additive mixed-effects models (GAMs) of FRP as a function of contemporaneous Canadian Fire Weather Index (FWI)[24], while accounting for other environmental variables that likely influence fire intensity (tree cover, leaf area index, slope, biome, biogeographic realm, ecoregion). FWI is a numeric rating of the influence of weather on fire behaviour calculated from consecutive daily observations of temperature, relative humidity, wind speed, and precipitation[24], and has been widely used to evaluate fire weather and risk around the world

[1]Fire Centre, School of Natural Sciences, University of Tasmania, Hobart, Australia. [2]Department of Management of Complex Systems, University of California, Merced, Merced, CA, USA. ✉e-mail: calum.cunningham@utas.edu.au

(e.g.[1,25,26]). Based on the statistical relationship between FWI and FRP, we then projected FRP under future fire weather. Future FWI was estimated using a pseudo climate change experiment that involved perturbing historical FWI values (2000–2023) by monthly pattern scaling[27] as derived from the multi-model median of 20 general circulation models (Supplementary Table 1). After projecting future fire intensity, we intersected maps of the estimated change in fire intensity with a recent map[14] of the WUI, allowing us to identify geographic concentrations of human exposure to increasing fire intensity over near-term horizons most relevant to decision making[28].

Results

Fire weather increases fire intensity

Fire weather was positively associated with fire intensity in all biomes, but response curves varied in steepness and curvature among biomes (Fig. 1). GAMs explained on average 30% of the deviance (range: 20–42%) in FRP, and FWI improved model fit for each biome (Supplementary Fig. 1). The steepest responses to FWI occurred in regions well-known for intense fires with high socio-economic costs[7,29], most notably, the Temperate Broadleaf Forest biome in Australia and South America, the Temperate Conifer Forest biome in North America, and the Mediterranean biome globally (Fig. 1). These steeper response curves imply that increases in fire weather may have more pronounced effects on fire intensity in those regions compared to regions with flatter response curves. The best-performing models (Supplementary Fig. 1) consistently revealed different effects of FWI at day and night, with nighttime FRP consistently lower (Supplementary Fig. 2). The best-performing proxy of fuel load varied by biome, with FRP best explained by leaf area index in seven biomes and by percent tree cover in the remaining six biomes (Supplementary Fig. 1).

Projected changes in fire weather and fire intensity

Projected fire weather under 1.5 °C and 2 °C warming (Supplementary Fig. 3) indicates that the number of days exceeding the 93rd percentile (2000–2023) of FWI (FWI_{93}) will increase by an average of 2.3 and 5.3 days per year globally (Supplementary Fig. 4), respectively. Increases were most pronounced outside the tropics (Supplementary Fig. 3), with the Mediterranean biome projected under 2 °C to have an additional 7.7 days per year above FWI_{93} (Supplementary Fig. 4). We focus here on FWI_{93} because it reflects potentially dangerous fire weather that would occur in most fire seasons (25th worst day in a year) and has been shown to be associated with energetically extreme fire events[7], but see Supplementary Fig. 6 for a comparison of other FWI percentiles.

Under the FWI projections, our models project that 88% (+1.5 °C) and 89% (+2 °C) of fire-prone (see Method) areas on Earth are likely to experience statistically significant increases in fire intensity (i.e., lower confidence bound for the projected difference > 0), while holding other predictors unchanged. Under 1.5 °C warming, FRP projections increased by a global mean of 0.69 MW/pixel (1%), with increases as large as 29.7 MW/pixel (7.1%) in the temperate broadleaf forests of South America. Increases were largest in the boreal forests, western North America, southern Amazonia, southern South America, Mediterranean Europe, southern Africa and southern Australia (Fig. 2b).

Patterns were similar but an average of 2.1-fold larger and up to 64.8 MW/pixel (15.6%) under 2 °C warming (Fig. 2c). The substantial increase from 1.5 °C to 2 °C highlights the importance of every prevented increment of warming. Substantial parts of these regions, such as the Amazon rainforest and boreal forests, contain intact forests of immense natural value with major carbon stores, while the remainder include the juxtaposition of flammable wildlands and urban areas (i.e., the WUI).

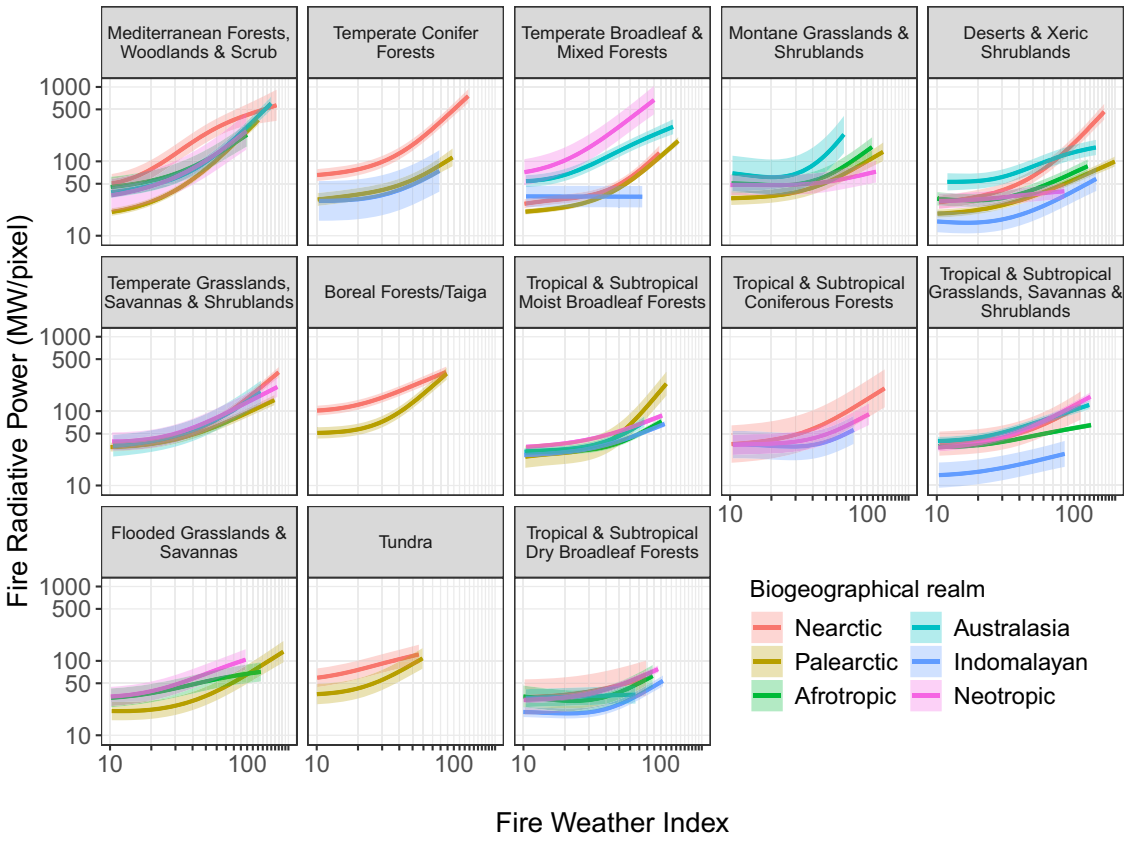

Fig. 1 | Fire weather index (FWI) is positively associated with fire radiative power (FRP). Lines show the fitted responses (±95% CI) from the GAMs, with all other predictors held at their realm-specific means. Panels are ordered from largest to smallest effect of FWI, measured by the difference between the maximum and minimum predictions of FRP in response to FWI. Lines show the fitted responses for daytime FRP, but see Supplementary Fig. 2 for a comparison of day and night responses to FWI. For visualisation purposes, axes are shown on the log scale, and the *x*-axis is truncated at 10.

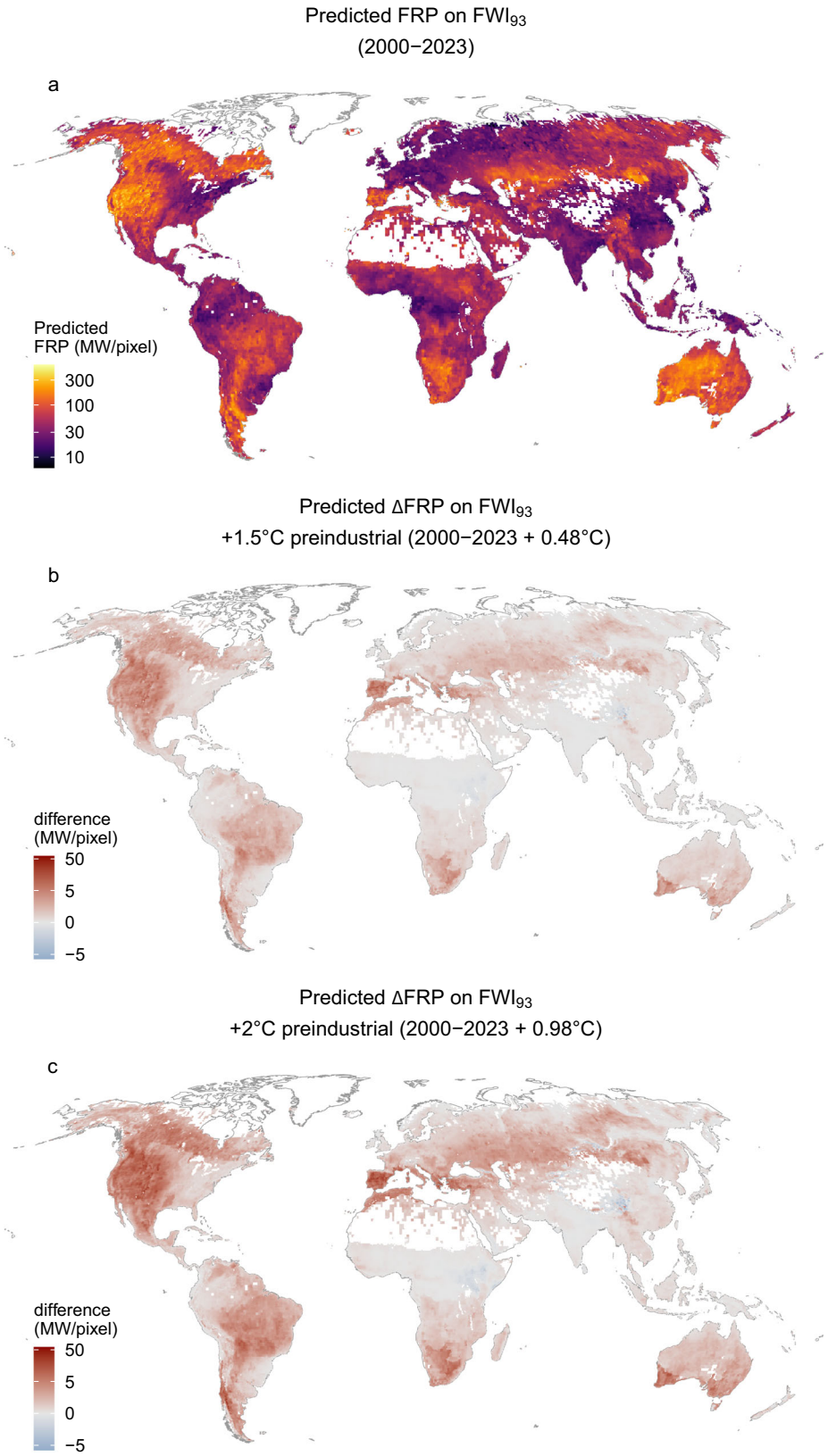

Fig. 2 | Increasing fire weather under climate change will lead to increasing fire radiative power. **a** Projected fire radiative power from the GAMs under FWI_{93} for the period (2000–2023) aligning with the MODIS active fire data. **b**, **c** The difference between projected FRP under FWI_{93} historical (2000–2023) and FWI_{93} with 1.5 °C and 2 °C warming above preindustrial levels (0.48 °C and 0.98 °C above 2000–2023). FWI projections were based on a pseudo climate change experiment involving the multi-model median of 20 general circulation models. For visualisation purposes, the colour scale of **a** is on the square root scale and **b**, **c** are on the asinh scale. Areas in white are outside of the fire-prone Earth (see Method).

Near-term increases in fire intensity in the wildland-urban interface

Intersecting a map of the WUI[14] with projected increases in fire intensity (Fig. 1c) identified several regions already known for their relatively high incidence of socially disastrous wildfires[29]—namely western North America, Chile, South Africa, Mediterranean Europe and southern Australia—as loci of substantial change (Fig. 3 and Supplementary Fig. 7). In support of this pattern, increases in projected fire intensity under 1.5 °C warming were 3.6 times larger at 159 WUI locations (reported by Cunningham et al.[29]) that have experienced major socioeconomic wildfire disasters from 1980 to 2023

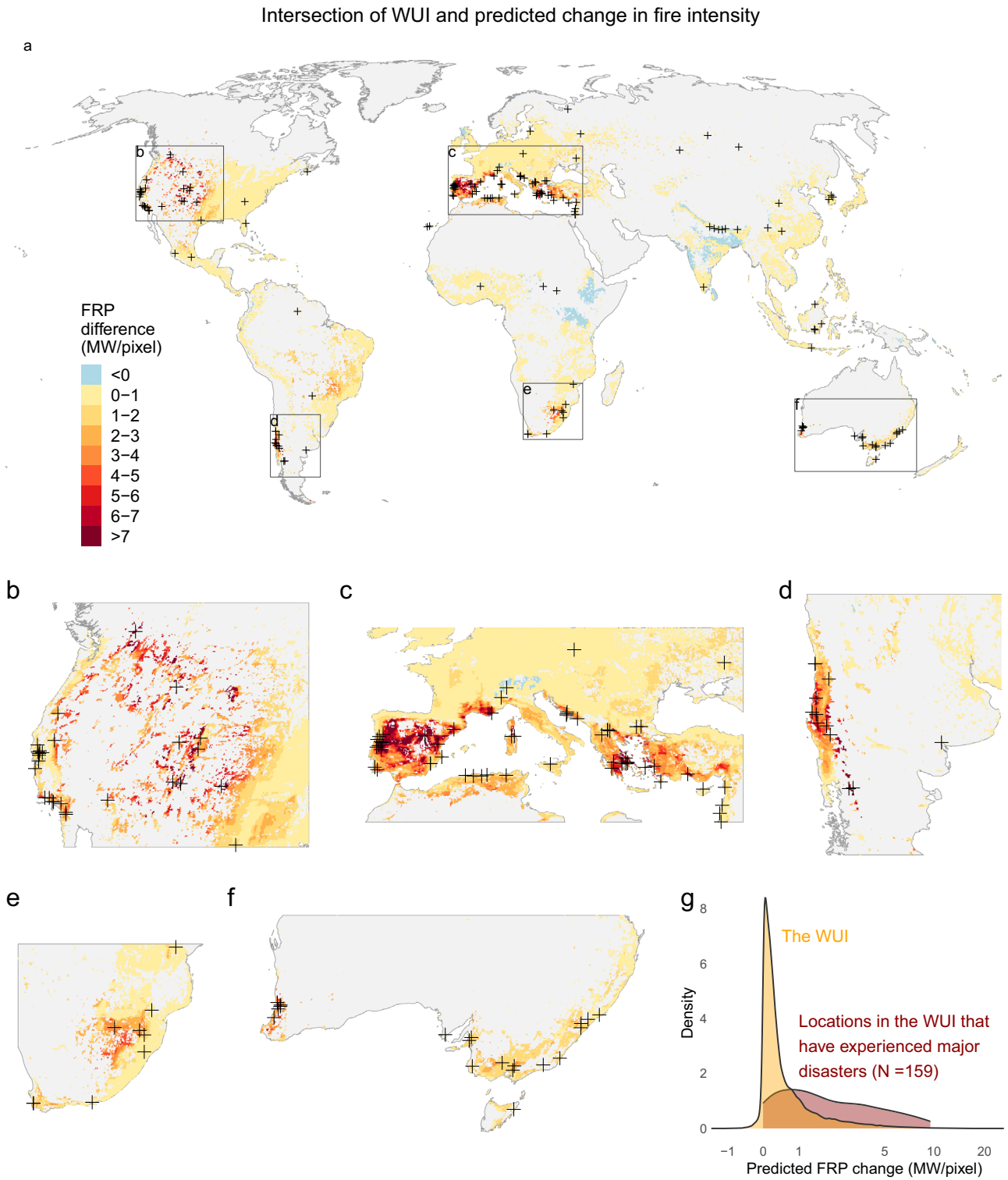

Fig. 3 | Projected change in fire intensity in the wildland-urban interface with 1.5 °C warming. a Projected change in FRP on FWI_{93} (Fig. 1c) was intersected with the estimated distribution of the wildland-urban interface in 2020[14]. Colours show areas of the WUI, and grey shows non-WUI. **b**–**f** Regions with the largest increases in projected FRP in the WUI. Crosses show 159 WUI disasters from a systematic dataset of major wildfire disasters from 1980 to 2023[29]. **g** Projected changes in fire intensity were larger in locations of the WUI that have experienced major wildfire disasters during the period 1980–2023 compared to the WUI more broadly, suggesting disaster-prone regions will be further exposed to disastrous fires. See Supplementary Fig. 7 for 2 °C warming.

compared to other areas of the WUI globally (mean of 2.42 MW/pixel vs 0.67 MW/pixel; two-sample Wilcoxon test $p < 0.00001$; Fig. 3g). This pattern implies that effects of wildfire in disaster-prone regions will become further exacerbated under near-term climate change.

Discussion

Fire intensity is rising in some ecosystems[11,12], making fires more destructive and difficult to control. Our analysis provides near-term projections of likely changes in wildfire intensity globally, suggesting that fire intensity will rise

across most of the Earth's fire-prone areas under warming scenarios of 1.5 °C—roughly reflecting the coming decade—and 2 °C. These changes were not evenly distributed, with the largest increases in FRP projected for regions that contain highly flammable ecosystems, such as the Mediterranean biome and the Temperate Conifer Forest biome. The Wildland–Urban Interface, as the locus of major wildfire disasters, is of profound importance for human adaptation to extreme wildfires[14,30–32]. Regions of the WUI already known for wildfire disasters[29] were projected to see disproportionate intensification of fire compared to other areas of the WUI, potentially amplifying the impacts of fire in places where consequences are already severe. These projections match emerging evidence of recent anomalous fire seasons or events, including in western Amazonia, Australia, Canada, Chile, France, Greece, Hawaii, Portugal, Siberia and the western United States[3,4,33–36].

It has been widely reported that fire weather will continue to increase with climate change[15,16], and our findings provide important new knowledge on how such changes will likely manifest in fire intensity. This can help focus attention on where fire behaviour, rather than fire weather, will change most. For example, although fire weather is projected to increase by a similar magnitude across the boreal forests (Supplementary Fig. 3), our models project that fire intensity will increase by a larger amount in North American boreal forests than European or Siberian boreal forests (Fig. 2b, c; Supplementary Fig. 5), aligning with analysis that suggests European boreal forests are less sensitive to changes in climate[37].

Although expected, projections of increasing fire intensity are concerning because fire suppression becomes increasingly difficult as fire intensity increases, pushing fires closer to exceeding suppression capacity[38,39]. While the projected increases may seem relatively modest, they are increments added to fires that are already difficult to contain. Because FRP is only expressed for fires that have already ignited, the projections of FRP must be interpreted as conditional on the presence of an ignition. If climate change, as expected, also drives changes in other aspects of fire regimes, such as ignition probability[15] and rate of spread[40], this means the projected increases in fire intensity are likely to occur alongside other changes that also make fires more difficult to control. Taken together, there is the very real risk that effective fire suppression is currently masking the potential for very destructive fires because such changes in already hazardous locations may push systems past critical thresholds, leading to disproportionate increases in damage[41].

Beyond suppression, increasing fire intensity will likely lead to increasing carbon emissions because fire intensity is directly proportional to biomass burned[6]. This is in line with an emerging trend of increasing carbon combustion efficiency[42] and emissions per unit area from fires[43]. It is also likely that intensifying fires will be more ecologically destructive. Our results are likely conservative because they focus only on changes to fire weather. If other climate-related effects act independently of fire weather and lead to higher fuel loads—such as CO_2-driven increases in primary productivity[22], drought-induced tree mortality[23], or windthrow[44]—then we might expect larger increases in fire intensity than those projected here.

We used the MODIS active fire dataset because it is the longest-running dataset on fire radiative power, indicating increases in energetically extreme fire events[13] and increasing nighttime fire intensity[11] over the last two decades. Active fires detected by MODIS can be substantially smaller than the 1 km^2 pixel[17], meaning there is inevitably some noise in matching fires to environmental variables. Future research could refine the spatio-temporal scale of analysis, thereby reducing various uncertainties. For instance, newer, finer-scale datasets of FRP, such as VIIRS (375 m resolution), should allow for tighter spatial matches between fires and land use. Moreover, newer geostationary satellites allow for higher temporal resolution linkage between fire intensity and weather, including using (e.g., hourly) fire weather indices based on regional climatologies (e.g., the McArthur Forest Fire Danger Index in Australia[45]). Such finer-grained analyses will also better characterise fireline intensities and more precisely resolve the effectiveness of mitigation and suppression efforts. As distinct from event-specific forecasts, which may be better modelled by fire propagation models, our outputs offer projections that can be used to anticipate and plan for broad-scale changes in future fire regimes over the coming decades.

Our results provide a global perspective on likely human vulnerability to extreme wildfire, thereby focusing on adaptation and mitigation strategies. We find that wildfire intensity will likely continue to increase in the near term, especially in already-vulnerable regions of the WUI, as well as regions with vast carbon stores such as the boreal and Amazon forests. Any increases in fire intensity in already-problematic regions will likely amplify the effects of fire, making fires that are already difficult to control even more so. This points to a critical research and development frontier in fire science and mitigation: managing ecosystems to reduce the intensity of wildfires[46]. Doing so will require major socio-ecological adaptation and innovation, including increasing the use of low-intensity prescribed fire and other preventative mitigation measures[47,48], allowing fires to burn under moderate conditions if it is safe to do so[38], and incorporating the wisdom of Indigenous use of low-intensity fire[49], at scales ranging from individual properties to broader landscapes[50].

Methods

The general workflow, including data processing, modelling, and projection, is summarised in Fig. 4. Analysis was conducted in R version 4.4.0[51], with package versions recorded in the "renv.lock" file included in the repository[52].

Data and data processing

The MODIS sensors on NASA's Terra and Aqua satellites identify active wildfires based on thermal anomalies. The MCD14ML product provides point locations of wildfire 'hotspots' at a resolution of 1 km, along with a measure of each hotspot's fire radiative power (FRP; megawatts). FRP has been widely used as a proxy of fire intensity and is very highly correlated with the rate of fuel mass combusted[6]. Hotspot locations represent the centre of a 1 km pixel that was identified as containing a fire somewhere within the pixel. We omitted observations flagged in the MODIS dataset as likely resulting from non-fire sources, and for additional robustness, we selected only high-confidence fires (i.e., confidence > 50)[17].

To explain and project the FRP of individual hotspots, we compiled 7 explanatory variables that we expected would influence fire intensity (Table 1). Six of these variables measure static and dynamic features of the environment, including slope, biogeography (biogeographical realm and biome), and proxies of fuel load (percentage tree cover, leaf area index). While fire history also influences fuel load, we did not attempt to include it as an explanatory variable because there are insufficient long-term global records of the time since last fire.

We used the Canadian Forest Fire Weather Index (FWI) system to reflect the fire conditions coinciding with each hotspot. FWI is a numeric rating of estimated fire intensity, calculated from consecutive daily observations of temperature, relative humidity, wind speed, and 24-h precipitation[24]. The Canadian FWI system has been widely used in analyses of fire risk and fuel moisture around the world (e.g.[25,26,53]). FWI was calculated using daily summaries of maximum temperature, relative humidity, wind speed, and 24-h precipitation from ERA5 reanalysis[54].

For each hotspot in the MODIS record between 2000 and 2023, we extracted FWI on the day of the fire and extracted temporally dynamic vegetation variables in the nearest year. Because the full MODIS dataset was excessively large for statistical modelling (n = ~103 million observations), we sub-sampled the dataset to reduce its size while ensuring broad spatial coverage; for 1-degree grid cells that had more than 500 hotspots, we randomly sampled 500 hotspots (separately for daytime and nighttime hotspots), and we retained all observations for grid cells that had fewer than 500 hotspots. This process ensured that all 1-degree grid cells containing a hotspot, which we consider the fire-prone Earth, were retained for analysis, while not unduly skewing the analysis to grid cells with superabundant data. While this threshold itself is arbitrary, it ensured a tractable amount of data for analysis, resulting in a dataset with 8.98 million hotspots used for model fitting.

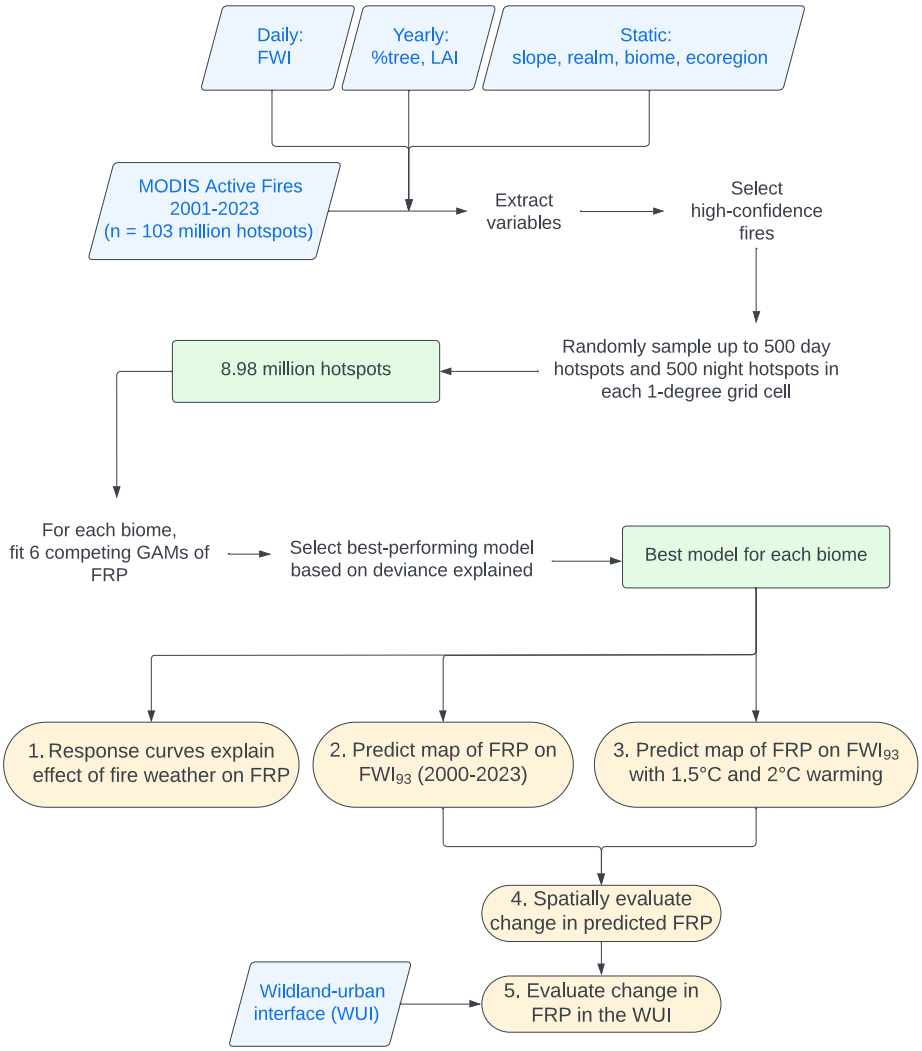

Fig. 4 | General workflow of data processing and analysis.

Statistical modelling of fire radiative power

We constructed generalised additive models (GAMs) that explained the fire radiative power of hotspots using the mgcv package version 1.9-1[55]. GAMs are like generalised linear models, except they can flexibly model non-linear effects, making them well-suited to revealing thresholds and non-linearities, such as whether there are thresholds of fire weather above which fire intensity increases sharply. We fitted the GAMs using the log-link Gamma distribution, which is well-suited to modelling positive, continuous, right-skewed data, such as FRP. We fitted separate GAMs for each biome because we expected fundamentally different relationships in each. For each biome, we fitted six competing models (see Supplementary Fig. 1 for model formulas), with the most complex model taking the form:

$$\begin{aligned} FRP \sim & f_1(log\,FWI,\ by = realm \times day/night) + f_2(logSlope) \\ & + f_3(vegetation) + realm + satellite + day/night \\ & + f_4(ecoregion, bs = random) + f_5(gridcell, bs = random) \end{aligned}$$

where f_1 indicates a smooth function of logFWI, differing for each combination of realm and day/night; f_2 is a smooth effect of logSlope; f_3 is a smooth effect of proxies of vegetative fuel (either %tree or LAI, transformed per Table 1); realm is a categorical effect that allows each realm to have its own baseline; satellite is a categorical term used to control for the effect of the different overpass times of the Terra and Aqua satellites; and day/night is a categorical effect of whether a hotspot observation occurred during the day or night, during which we would expect differences in intensity. Random intercepts for ecoregion were included to account for possible differences in fire intensities among ecoregions within each biome, and random intercepts for each 1-degree grid cell were included to account for other unmodelled local effects on fire radiative power and control for likely similarities in hotspots occurring in the same cell.

To prevent overly complex (i.e., wiggly) response shapes, the complexity of smooth functions was restricted in line with our a priori expectations ($k = 5$). Furthermore, to prevent overfitting, we fit the model using thin plate regression splines with additional smoothing penalties, allowing the term to be shrunk to zero if there is no evidence for an effect[55]. Models were ranked based on their explanatory power by comparing the deviance explained by each (Supplementary Fig. 1).

Projecting fire intensity under near-term climate projections

Using the best-performing model for each biome, we projected FRP under near-term projected fire weather. Fire weather index was projected using a pseudo climate change experiment approach that perturbs the observed daily temperature, wind speed, relative humidity, and precipitation using climate model results. Specifically, we apply a pattern scaling approach[27] that scales local changes in each climate variable to first-order changes in climate as in prior studies[7,56]. We used 20 climate models participating in CMIP6 (Supplementary Table 1) that had daily maximum temperature, minimum relative humidity, precipitation, and 10-m daily mean wind speed. For each model we calculated differences in monthly mean variables aggregated to a

Table 1 | Description of explanatory variables used to model fire radiative power

Variables	Description and reference	Resolution (time; space)
Fire weather		
logFWI	Fire Weather Index, representing a numeric rating of the influence of weather on fire behaviour, calculated from ERA5 global reanalysis[54]. Data were log(FWI + 1) transformed to reduce the influence of large outliers (i.e., reduce positive skew).	Daily; 0.25°
Environment		
%tree	% tree cover (0–100) from MODIS (product MOD44B)[57], providing a proxy of the amount of vegetative fuel load.	Annual; summarised at 1 km
LAI	Leaf area index from MODIS (product MCD15A3H)[58], providing a proxy of vegetation fuel load. LAI is defined as one-sided green leaf area per unit ground in broadleaf canopies and as half of the total needle surface area per unit ground in coniferous canopies.	Annual; summarised at 1 km
Realm	Biogeographical realms as described by Dinerstein et al.[59] ecoregions of the world.	Static; polygons
Biome	Biomes as described by Dinerstein et al.[59] ecoregions of the world.	Static; polygons
Ecoregion	Ecoregions as described by Dinerstein et al.[59] ecoregions of the world.	Static; polygons
logSlope	Slope in degrees. Slope was derived by Amatulli et al.[60] from a global digital elevation model GMTED at 250-m resolution;[61]. Data were log-transformed before modelling to reduce the influence of outliers.	Static; 1 km

common 1-degree horizontal grid between the 1850–1900 quasi-preindustrial baseline using historical forcing and 2041–2070 using SSP2-45 forcing. Monthly scale factors were defined as the differences between the two periods divided by the difference in global mean temperature. These patterns assume a linear response between local changes in climate for each variable and the amount of global warming and allow us to recast projections relative to the amount of global warming in a scenario-agnostic way. While this approach does not capture attributes of changing variability, it provides a sensible way to perturb observed meteorological forcing that can be seamlessly compared with the observed record. We recalculate FWI using the same procedures using the perturbed meteorological data for +1.5 °C and +2 °C, representing 0.48 °C and 0.98 °C above the period 2000–2023.

Based on the modelled relationships between FRP and FWI, we projected FRP under near-term FWI. Specifically, we used the GAMs to project FRP on 93rd percentile FWI for the period 2000–2023, and with 1.5 °C and 2 °C warming above preindustrial conditions. This threshold of FWI_{93} represents the ~25th worst FWI day in an average year, reflecting potentially dangerous fire conditions that would occur in most fire seasons. This threshold corresponds with the fire weather coinciding with a majority of energetically extreme fire events[7]. In addition to focusing on FWI_{93}, we also provide a supplementary comparison of projected FRP on FWI_{95}, $FWI_{97.5}$ and FWI_{99}. We produced maps of the difference (megawatts) between projected daytime FRP under historical weather and FRP under the warming scenarios at a resolution of 0.09° (~10 km).

To characterise human exposure to increasing fire intensity, we intersected the map of change in FRP with a map of the wildland-urban interface and intermix in 2020[14], considering those sub-categories together as the wildland urban interface (WUI). Furthermore, to evaluate projected change in FRP in disaster-prone areas of the WUI, we used the locations of major disasters reported by a systematic analysis of major disasters from 1980 to 2023[29], defined as events that caused 10 or more fatalities or the 200 largest economic events relative to a country's gross domestic product at the time. From these events, we selected those intersecting the WUI ($n = 159$ disasters). We used a two-sample Wilcoxon test to compare projected change in FRP at these disaster-prone locations with the rest of the WUI.

Reporting summary

Further information on research design is available in the Nature Portfolio Reporting Summary linked to this article.

Data availability

Pre-processed data and model projections are archived at https://doi.org/10.6084/m9.figshare.28711454[52]. MODIS active fire records used in the analysis are publicly available and were downloaded from the University of Maryland ftp server (sftp://fuoco.geog.umd.edu). Biomes of the world were downloaded from https://ecoregions.appspot.com/. Disaster locations from Cunningham, et al.[29] were largely based on the NatCatSERVICE dataset (contact: https://www.munichre.com/en/solutions/reinsurance-property-casualty/natcatservice.html) provided to us in 2018 by Munich Reinsurance Company under a contractual condition prohibiting us from sharing this commercially confidential dataset.

Code availability

Code is archived at https://doi.org/10.6084/m9.figshare.28711454[52].

Received: 1 December 2024; Accepted: 11 June 2025;
Published online: 09 July 2025

References

1. Abatzoglou, J. T., Williams, A. P. & Barbero, R. Global emergence of anthropogenic climate change in fire weather indices. *Geophys. Res. Lett.* **46**, 326–336 (2019).
2. Canadell, J. G. et al. Multi-decadal increase of forest burned area in Australia is linked to climate change. *Nat. Commun.* **12**, 6921 (2021).
3. Jain, P. et al. Drivers and impacts of the record-breaking 2023 wildfire season in Canada. *Nat. Commun.* **15**, 6764 (2024).
4. Abram, N. J. et al. Connections of climate change and variability to large and extreme forest fires in southeast Australia. *Commun. Earth Environ.* **2**, 8 (2021).
5. Keeley, J. E. Fire intensity, fire severity and burn severity: a brief review and suggested usage. *Int. J. Wildland Fire* **18**, 116–126 (2009).
6. Wooster, M. J., Roberts, G., Perry, G. L. W. & Kaufman, Y. J. Retrieval of biomass combustion rates and totals from fire radiative power observations: FRP derivation and calibration relationships between biomass consumption and fire radiative energy release. *J. Geophys. Res.* https://doi.org/10.1029/2005JD006318 (2005).
7. Bowman, D. M. J. S. et al. Human exposure and sensitivity to globally extreme wildfire events. *Nat. Ecol. Evolut.* **1**, 0058 (2017).
8. Moritz, M. A. et al. Learning to coexist with wildfire. *Nature* **515**, 58–66 (2014).
9. Kaiser, J. W. et al. Biomass burning emissions estimated with a global fire assimilation system based on observed fire radiative power. *Biogeosciences* **9**, 527–554 (2012).
10. Haas, O., Prentice, I. C. & Harrison, S. P. Global environmental controls on wildfire burnt area, size, and intensity. *Environ. Res. Lett.* **17**, 065004 (2022).
11. Balch, J. K. et al. Warming weakens the night-time barrier to global fire. *Nature* **602**, 442–448 (2022).
12. Yang, X., Zhao, C., Zhao, W., Fan, H. & Yang, Y. Characterization of global fire activity and its spatiotemporal patterns for different land cover types from 2001 to 2020. *Environ. Res.* **227**, 115746 (2023).

13. Cunningham, C. X., Williamson, G. J. & Bowman, D. M. J. S. Increasing frequency and intensity of the most extreme wildfires on Earth. *Nat. Ecol. Evolut.* https://doi.org/10.1038/s41559-024-02452-2 (2024).
14. Chen, B. et al. Wildfire risk for global wildland–urban interface areas. *Nat. Sustain.* **7**, 474–484 (2024).
15. Clarke, H. et al. Forest fire threatens global carbon sinks and population centres under rising atmospheric water demand. *Nat. Commun.* **13**, 7161 (2022).
16. Jones, M. W. et al. Global and regional trends and drivers of fire under climate change. *Rev. Geophys.* **60**, e2020RG000726 (2022).
17. Giglio, L., Schroeder, W., Hall, J. & Justice, C. *MODIS Collection 6 Active Fire Product User's Guide Revision B* (NASA, 2018).
18. Arias, P. A. et al. Technical Summary. In Climate Change 2021: The Physical Science Basis. Contribution of Working Group I to the Sixth Assessment Report of the Intergovernmental Panel on Climate Change [Masson-Delmotte, V., P. Zhai, A. Pirani, S. L. Connors, C. Péan, S. Berger, N. Caud, Y. Chen, L. Goldfarb, M. I. Gomis, M. Huang, K. Leitzell, E. Lonnoy, J. B. R. Matthews, T. K. Maycock, T. Waterfield, O. Yelekçi, R. Yu, and B. Zhou (eds.)]. Cambridge University Press, Cambridge, United Kingdom and New York, NY, USA, 33–144. https://doi.org/10.1017/9781009157896.002 (2021).
19. Hausfather, Z. & Peters, G. P. Emissions–the 'business as usual'story is misleading. *Nature* **577**, 618–620 (2020).
20. Bowman, D. M. J. S., Murphy, B. P., Williamson, G. J. & Cochrane, M. A. Pyrogeographic models, feedbacks and the future of global fire regimes. *Glob. Ecol. Biogeogr.* **23**, 821–824 (2014).
21. Le Breton, T. D. et al. Megafire-induced interval squeeze threatens vegetation at landscape scales. *Front. Ecol. Environ.* **20**, 327–334 (2022).
22. Zhu, Z. et al. Greening of the Earth and its drivers. *Nat. Clim. Change* **6**, 791–795 (2016).
23. Brodribb, T. J., Powers, J., Cochard, H. & Choat, B. Hanging by a thread? Forests and drought. *Science* **368**, 261–266 (2020).
24. Wagner, C. V. *Development and Structure of the Canadian Forest Fire Weather Index System*. (1987).
25. Abatzoglou, J. T., Williams, A. P., Boschetti, L., Zubkova, M. & Kolden, C. A. Global patterns of interannual climate–fire relationships. *Glob. Change Biol.* **24**, 5164–5175 (2018).
26. Carvalho, A., Flannigan, M. D., Logan, K., Miranda, A. I. & Borrego, C. Fire activity in Portugal and its relationship to weather and the Canadian Fire Weather Index System. *Int. J. Wildland Fire* **17**, 328–338 (2008).
27. Tebaldi, C. & Arblaster, J. M. Pattern scaling: Its strengths and limitations, and an update on the latest model simulations. *Clim. Change* **122**, 459–471 (2014).
28. Nissan, H. et al. On the use and misuse of climate change projections in international development. *WIREs Clim. Change* **10**, e579 (2019).
29. Cunningham, C. X. et al. Climate-linked escalation of societally disastrous wildfires. *EcoEvoRxiv* https://doi.org/10.32942/X22622 (2024).
30. Kumar, M., AghaKouchak, A., Abatzoglou, J. T. & Sadegh, M. Compounding effects of climate change and WUI expansion quadruple the likelihood of extreme-impact wildfires in California. *npj Nat. Hazards* **2**, 17 (2025).
31. Calkin, D. E. et al. Wildland-urban fire disasters aren't actually a wildfire problem. *Proc. Natl Acad. Sci. USA* **120**, e2315797120 (2023).
32. Radeloff, V. C. et al. Rapid growth of the US wildland-urban interface raises wildfire risk. *Proc. Natl Acad. Sci. USA* **115**, 3314–3319 (2018).
33. Jones, M. W. et al. State of Wildfires 2023–2024. *Earth Syst. Sci. Data* **16**, 3601–3685 (2024).
34. Carrasco-Escaff, T., Garreaud, R., Bozkurt, D., Jacques-Coper, M. & Pauchard, A. The key role of extreme weather and climate change in the occurrence of exceptional fire seasons in south-central Chile. *Weather Clim. Extremes* **45**, 100716 (2024).
35. Bowman, D. M. J. S. et al. Vegetation fires in the Anthropocene. *Nat. Rev. Earth Environ.* **1**, 500–515 (2020).
36. Turco, M. et al. Climate drivers of the 2017 devastating fires in Portugal. *Sci. Rep.* **9**, 13886 (2019).
37. Scholten, R. C., Veraverbeke, S., Chen, Y. & Randerson, J. T. Spatial variability in Arctic–boreal fire regimes influenced by environmental and human factors. *Nat. Geosci.* **17**, 866–873 (2024).
38. Kreider, M. R. et al. Fire suppression makes wildfires more severe and accentuates impacts of climate change and fuel accumulation. *Nat. Commun.* **15**, 2412 (2024).
39. Fried, J. S. et al. Predicting the effect of climate change on wildfire behavior and initial attack success. *Clim. Change* **87**, 251–264 (2008).
40. Balch, J. K. et al. The fastest-growing and most destructive fires in the US (2001 to 2020). *Science* **386**, 425–431 (2024).
41. Arévalo, J. R. & Naranjo-Cigala, A. Wildfire Impact and the "Fire Paradox" in a Natural and Endemic Pine Forest Stand and Shrubland. *Fire* https://mdpi-res.com/d_attachment/fire/fire-01-00044/article_deploy/fire-01-00044.pdf?version=1542107456 (2018).
42. Jones, M. W. et al. Global rise in forest fire emissions linked to climate change in the extratropics. *Science* **386**, eadl5889 (2024).
43. Zheng, B. et al. Increasing forest fire emissions despite the decline in global burned area. *Sci. Adv.* **7**, eabh2646 (2021).
44. Fairman, T. A., Symon, C., Cawson, J. & Penman, T. D. Throwing fuel on the fire? Contrasting fine and coarse fuel responses to windthrow in temperate eucalypt forests in south-eastern Australia. *For. Ecol. Manag.* **572**, 122266 (2024).
45. McArthur, A. G. Fire behaviour in Eucalypt forests. Department of National Development, Forestry and Timber Bureau Leaflet No. 107. Canberra, Australia. (1967).
46. Bowman, D. M. J. S. Pathways for sustainable coexistence with wildfires. *Nature Sustain* **7**, 1547–1549 (2024).
47. Kolden, C. A. We're not doing enough prescribed fire in the Western United States to mitigate wildfire risk. *Fire* https://mdpi-res.com/d_attachment/fire/fire-02-00030/article_deploy/fire-02-00030.pdf?version=1559117001 (2019).
48. Wu, X., Sverdrup, E., Mastrandrea, M. D., Wara, M. W. & Wager, S. Low-intensity fires mitigate the risk of high-intensity wildfires in California's forests. *Sci. Adv.* **9**, eadi4123 (2023).
49. Steffensen, V. Fire country: how Indigenous fire management could help save Australia. (2020).
50. Bowman, D. M. J. S. & Sharples, J. J. Taming the flame, from local to global extreme wildfires. *Science* **381**, 616–619 (2023).
51. R: A Language and Environment for Statistical Computing (R Foundation for Statistical Computing, Vienna, Austria, 2023).
52. Cunningham, C. Projecting Fire Intensity: data and code. *figshare* https://doi.org/10.6084/m9.figshare.28711454.v1 (2025).
53. Ellis, T. M., Bowman, D. M. J. S., Jain, P., Flannigan, M. D. & Williamson, G. J. Global increase in wildfire risk due to climate-driven declines in fuel moisture. *Glob. Change Biol.* **28**, 1544–1559 (2022).
54. Hersbach, H. et al. The ERA5 global reanalysis. *Q. J. R. Meteorol. Soc.* **146**, 1999–2049 (2020).
55. Wood, S. N. *Generalized Additive Models: An Introduction with R (2nd ed.)*. (CRC Press, 2017).
56. Abatzoglou, J. T., Dobrowski, S. Z. & Parks, S. A. Multivariate climate departures have outpaced univariate changes across global lands. *Sci. Rep.* **10**, 3891 (2020).
57. DiMiceli, C. et al. MOD44B MODIS/Terra Vegetation Continuous Fields Yearly L3 Global 250m SIN Grid V006 [Dataset]. NASA EOSDIS Land Processes Distributed Active Archive Center. Accessed 2024-09-10 from https://doi.org/10.5067/MODIS/MOD44B.006. (2015).
58. Myneni, R., Knyazikhin, Y., Park, T. MODIS/Terra+Aqua Leaf Area Index/FPAR 4-Day L4 Global 500m SIN Grid V061 [Data set]. NASA EOSDIS Land Processes Distributed Active Archive Center. Accessed

2025-03-24 from https://doi.org/10.5067/MODIS/MCD15A3H.061. (2021).
59. Dinerstein, E. et al. An Ecoregion-based approach to protecting half the terrestrial realm. *BioScience* **67**, 534–545 (2017).
60. Amatulli, G. et al. A suite of global, cross-scale topographic variables for environmental and biodiversity modeling. *Sci. Data* **5**, 180040 (2018).
61. Danielson, J. J. & Gesch, D. B. Global multi-resolution terrain elevation data 2010 (GMTED2010). Report No. 2331-1258, (US Geological Survey, 2011).

Acknowledgements

This research was funded by the Australian Government through an Australian Research Council Laureate Fellowship (FL220100099) awarded to DMJSB, which also supports CXC and GJW. JTA was supported by NSF award OAI-2019762.

Author contributions

Conceptualisation: C.X.C. and D.M.J.S.B.; Methodology: C.X.C., J.T.A. and T.M.E.; Data: C.X.C., J.T.A. and T.M.E.; Investigation: C.X.C., J.T.A. and T.M.E.; Visualisation: C.X.C.; Funding acquisition: D.M.J.S.B.; Supervision: D.M.J.S.B.; Writing—original draft: C.X.C.; Writing—review & editing: C.X.C., D.M.J.S.B., J. T.A., G.J.W. and T.M.E.

Competing interests

The authors declare no competing interests.

Additional information

Supplementary information The online version contains supplementary material available at https://doi.org/10.1038/s43247-025-02475-y.

Correspondence and requests for materials should be addressed to Calum X. Cunningham.

Peer review information *Communications Earth & Environment* thanks Shengbiao Wu, Ana Freitas and Binbin He for their contribution to the peer review of this work. Primary Handling Editors: Mengjie Wang. A peer review file is available.